

Theaflavins Depolymerize Microtubule Network through Tubulin Binding and Cause Apoptosis of Cervical Carcinoma HeLa Cells

Subhendu Chakrabarty, Amlan Das, Abhijit Bhattacharya, and Gopal Chakrabarti*

Department of Biotechnology and Dr. B. C. Guha Centre for Genetic Engineering and Biotechnology, University of Calcutta, 35 Ballygunge Circular Road, Kolkata, WB 700019, India

ABSTRACT: Here we studied the antiproliferative activity of theaflavins in cervical carcinoma HeLa cells by investigating their effects on cellular microtubules and purified goat brain tubulin. Theaflavins inhibited proliferation of HeLa cells with IC_{50} value of $110 \pm 2.1 \mu\text{g/mL}$ ($p < 0.01$), caused cell cycle arrest at G_2/M phase and induced apoptosis with alteration of expression of pro- and antiapoptotic proteins. Along with these antiproliferative activities, theaflavins act as microtubule depolymerizers. Theaflavins disrupted the microtubule network accompanied by alteration of cellular morphology and also decreased the polymeric tubulin mass of the cells. The polymerization of cold treated depolymerized microtubules in HeLa cells was prevented in the presence of theaflavins. *In vitro* polymerization of purified tubulin into microtubules was also inhibited by theaflavins with an IC_{50} value of $78 \pm 2.43 \mu\text{g/mL}$ ($P < 0.01$). Thus, disruption of cellular microtubule network of HeLa cells through microtubule depolymerization may be one of the possible mechanisms of antiproliferative activity of theaflavins.

KEYWORDS: theaflavins, microtubules network, apoptosis, anticancer activity, cell cycle

INTRODUCTION

Black tea is a promising agent for the chemoprevention of cancer.^{1,2} Although epidemiological studies concerning the relationship between tea consumption and cancer risk have been inconclusive,³ inhibition of carcinogenesis by black tea has been demonstrated in many animal models, including those involving cancers of the lung, skin, colon, esophagus and stomach.^{1,2,4} Theaflavins (TF), the bioactive polyphenols of black tea, exert anticancer activity by inducing apoptosis.^{5,6} Treatment with TF results in cell cycle arrest either in G_0/G_1 phase^{7,8} or in G_2/M phase.⁹ Theaflavins modulate pro- and antiapoptotic proteins^{7,9} and inhibit growth and proliferation of cancer cells.⁸

Tubulin, a heterodimeric (containing α and β subunits) protein, is polymerized to form microtubule, which has a versatile functions in cells, like cell division, maintenance of cell shape and structure, cell signaling and organelle transport.^{10,11} Microtubules are dynamic in nature, and it was established that this dynamicity is responsible for functions of microtubules. Dynamic equilibrium of tubulin–microtubule is among the popular targets for anticancer therapy. Based on the mechanism of action of alternation of microtubule dynamics, drugs can be classified into two categories. One group of drugs, like paclitaxel and docetaxel, stabilizes microtubule polymer, and the other group, like vinblastine and vincristine, inhibits tubulin polymerization into microtubule.^{12–14} All these microtubule inhibitors and various other tubulin binding agents perturb spindle microtubule function and arrest cell cycle at G_2/M phase.^{15–17}

So far, all studies reported with TF were performed either *in vivo* or in cancer cells under culture conditions, but there is no report about the effect of TF on cellular cytoskeleton protein. In the present study, we examined the antiproliferative effects of TF against HeLa cells (cervical carcinoma cells) in relation to their ability to depolymerize cellular microtubule and perturb tubulin assembly, *in vitro*. We chose cervical carcinoma cells because

there is no previous report on the effect of TF on cervical carcinoma although it is one of the most common forms of cancer in women.

MATERIALS AND METHODS

Chemicals. Dulbecco's minimal essential media (DMEM), fetal bovine serum (FBS), penicillin–streptomycin, trypsin, and amphotericin B were purchased from HyClone, Logan, UT, USA. Human cervical carcinoma cells (HeLa) were obtained from National Centre for Cell Science, Pune, India. DAPI, mouse monoclonal anti- α -tubulin antibody (raised in mouse), anti-mouse rhodamine conjugated IgG antibody, anti-mouse HRP-conjugated IgG antibody, guanosine-5'-triphosphate (GTP), piperazine-1,4-bis(2-ethanesulfonic acid) (PIPES), $MgCl_2$, ethylene glycol tetraacetic acid (EGTA), and theaflavins were purchased from SIGMA, St. Louis, MO, USA. Annexin V-FITC apoptosis detection kit was obtained from BD Biosciences, Franklin Lakes, NJ, USA. Other primary antibodies (against p53, Bax, Bcl-2, caspase-3) were purchased from Santa Cruz Biotechnology. The Bradford Protein estimation kit was purchased from Genei, India. All other chemicals and reagents were of analytical grade and purchased from Sisco Research Laboratories, India.

Cell Culture. Human cervical carcinoma cells (HeLa) were maintained in DMEM medium supplemented with 1 mM L-glutamine, 10% fetal bovine serum, 50 $\mu\text{g/mL}$ penicillin, 50 $\mu\text{g/mL}$ streptomycin and 2.5 $\mu\text{g/mL}$ amphotericin B. Cells were cultured at 37 °C in a humidified atmosphere containing 5% CO_2 . Cells were grown in tissue culture flasks until they were 80% confluent before trypsinization with 1 \times trypsin and splitting. The morphology of control and treated cells was observed by Olympus inverted microscope model CKX41.

Received: November 1, 2010

Accepted: January 11, 2011

Revised: January 3, 2011

Published: February 16, 2011

TF Treatment. Dry powder of TF was directly dissolved in 100% DMSO. In cell biology experiments, doses of TF were applied from secondary solution prepared by diluting the stock solution in PBS and the concentration of the secondary stock was maintained in such that effective DMSO concentration was always less than 1%. The untreated control cells contained the vehicle (1% DMSO). All *in vitro* experiments were done preparing secondary solutions in PEM buffer (50 mM PIPES, 1 mM EGTA, 1 mM MgSO₄, pH 7) where final DMSO concentration was less than 1%.

Cell Viability Assay (MTT Assay). The effect of TF on the viability of HeLa cells was determined with the MTT (3-[4,5-dimethylthiazol-2-yl]-2,5-diphenyltetrazolium bromide) assay.¹⁸ HeLa cells were plated in 96-well culture plate (1 × 10⁴ cells per well) and treated with various concentrations of TF (0–200 μg/mL) for both 24 and 48 h. Each concentration of TF was repeated in ten wells. MTT (5 mg/mL) was dissolved in PBS and filter sterilized, and then 20 μL of the prepared solution was added to each well. This was incubated until purple precipitate was visible. Subsequently, 100 μL of Triton-X was added and incubated in the well under darkness for 2 h at room temperature. The absorbance was measured on an ELISA reader (MultiskanEX, Lab systems, Helsinki, Finland) at a test wavelength of 570 nm and a reference wavelength of 650 nm. Data was calculated as the percentage of viable cells by the following formula:

$$\% \text{ viable} = [(A_t / A_s) \times 100]\%$$

A_t and A_s indicated the absorbance of the test substances and solvent control, respectively. Data was analyzed by plotting percent of viable cells against TF concentration, where the control cells were considered 100% viable. IC₅₀ was calculated from three such experiments by observing 50% reduction in cell viability from the curves obtained by using MS Excel.

Cell Cycle Analysis by Flow Cytometry. HeLa cells were grown at a density of 1 × 10⁶ cells/mL in 35 mm culture plate and then treated with different concentrations of TF (0–150 μg/mL) for 24 h. The cells were harvested and fixed in ice chilled methanol for at least 30 min in 4 °C. Cells were centrifuged from the fixative and suspended in PBS. Then RNase (100 μg/mL) was added and the cells were incubated for 4 h at 37 °C. After incubation 50 μg/mL PI was added and incubated for 30 min at 4 °C. Cell cycle analysis was performed using the Becton Dickinson FACScan, and the data was analyzed using the CellQuest program from Becton Dickinson. For each sample, 10,000 cells were counted. Cell cycle distribution was analyzed by gating the living populations.

Detection of Apoptosis by Flow Cytometer. Apoptosis was measured using flow cytometry by quantifying detectable phosphatidylserine on the outer membrane of apoptotic cells.¹⁹ Around 1 × 10⁵ HeLa cells were grown in 35 mm culture plate and were treated with TF (0–150 μg/mL) for 48 h. Cells were then stained for 15 min at room temperature in the dark with fluorescein isothiocyanate (FITC)-conjugated annexin V (1 μg/mL) and propidium iodide (PI) (0.5 μg/mL) in a Ca²⁺-enriched binding buffer. Annexin V-FITC and PI emissions were detected in the FL1 and FL2 channels of a FACS Calibur flow cytometer, using emission filters of 525 and 575 nm, respectively. The annexin V negative/PI negative population (lower left quadrant) was regarded as normal healthy cells, while annexin V positive/PI negative (lower right quadrant) and annexin V positive/PI positive (upper right quadrant) populations were taken as the measure of early apoptotic population and late apoptotic population, respectively. For each sample, 10,000 cells were gated and counted. Apoptosis analysis was performed using the Becton Dickinson FACScan and the data were analyzed using CellQuest program from Becton Dickinson.

Detection of Apoptosis by Confocal Microscopy. HeLa cells were cultured over glass coverslips in 35 mm plates to 60–70% confluence and then treated with different concentrations of TF

(0–150 μg/mL) for 48 h. Then the cells were stained with annexin V-FITC to label the phosphatidylserine at the outer membrane of the cells. Untreated cells did not bind annexin V-FITC for the presence of intact membrane. Apoptotic cells bound to annexin V-FITC due to the externalization of membrane phosphatidylserine.

Western Blot Analysis To Determine Pro- and Antiapoptotic Proteins. Western blot analysis was done to determine the expression level of p53, Bax, Bcl-2 and cleaved caspase-3 in TF treated and untreated HeLa cells. Cells were treated with different concentrations of TF (0–200 μg/mL) for 48 h. Then the cells were harvested, washed with cold PBS (pH-7.4) and lysed with ice-cold lysis buffer (50 mM Tris-HCl, 150 mM NaCl, 1 mM EGTA, 20 mM NaF, 100 mM Na₃VO₄, 1% NP 40, 1 mM PMSF, 10 μg/mL aprotinin and 10 μg/mL leupeptin, pH 7.4) for 30 min and centrifuged at 12000g for 30 min at 4 °C. The protein concentration of the clear supernatant was measured by Bradford method²⁰ using bovine serum albumin as standard. Protein samples (50 μg) were resolved on 10% SDS-PAGE followed by electrotransfer onto poly vinylidene difluoride membranes. The blots were blocked overnight with 5% skimmed milk. In separate experimental sets, the membrane was incubated with mouse monoclonal anti-p53 antibody (1:1000 dilution), mouse monoclonal anti-Bax antibody (1:1000 dilution), mouse monoclonal anti-Bcl-2 antibody (1:1000 dilution), mouse monoclonal anti-cleaved caspase-3 antibody (1:1000 dilution) and mouse monoclonal anti-β-actin antibody (1:1000 dilution) for 4 h at room temperature. After washing with tris-buffered saline containing 0.1% Tween-20, the membranes were then incubated with HRP conjugated anti-mouse secondary antibody (1:2000 dilution, Santa Cruz Biotechnology). The protein bands were visualized using chemiluminescence kit from Thermo Scientific, and the bands were quantified densitometrically in a Typhoon Trio variable mode imager from Amersham Biosciences using the software ImageQuant TL.

Determination of Mitochondrial Membrane Potential (Δψ). HeLa cells were treated with TF (50–150 μg/mL) for 48 h, and the untreated and TF treated HeLa cells were incubated with rhodamine 123 (5 μg/mL) for 60 min in the dark at 37 °C, harvested and suspended in PBS. The mitochondrial membrane potential was measured using flow cytometry by measuring the fluorescence intensity (FL-1, 530 nm) of 10,000 cells. Fluorescence intensity of three such experiments was measured, and the percent of mean fluorescence intensity (%MFI) was plotted against TF doses.

Sample Preparation for Confocal Microscopy. HeLa cells were cultured on coverslips at a density of 1 × 10⁵ cells/mL and incubated in the presence of different doses of TF (0–150 μg/mL) for 24 h. Subsequently cells were washed with PBS, fixed with 2% paraformaldehyde and permeabilized with cell permeable solution (0.1% Na-Citrate, 0.1% Triton). Nonspecific binding sites were blocked by incubating the cells with 5% BSA. Cells were then incubated with mouse monoclonal anti-α-tubulin antibody (1:200 dilutions) followed by anti-mouse rhodamine conjugated IgG antibody (1:150 dilutions) and DAPI (1 μg/mL). After incubation, cells were washed with PBS and viewed under a Zeiss LSM 510 Meta confocal microscope.

Western Blot Analysis To Determine Soluble and Polymerized Tubulin in TF Treated HeLa Cells. The cellular tubulin polymerization was quantified by a modified method which was originally described by Minotti et al.²¹ Cultured HeLa cells were treated with different concentrations of TF (100, 150 μg/mL) and 2 μM colchicine (positive control) for 24 h. Then the cells were washed twice with PBS and harvested by trypsinization. Cells were lysed at 37 °C for 5 min in the dark with 100 μL of hypotonic lysis buffer [1 mM MgCl₂, 2 mM EGTA, 0.5% NP-40, 20 μg/mL aprotinin, 20 μg/mL leupeptin, 1 mM orthovanadate, 2 mM PMSF, and 20 mM Tris-HCl (pH6.8)]. After a brief but vigorous vortex, the samples were centrifuged at 14000 rpm (21000g) for 10 min. The 100 μL supernatants containing soluble (cytosolic) tubulin were separated from the pellets containing polymerized

(cytoskeletal) tubulin. The pellets were resuspended in 100 μL of lysis buffer. The total concentrations of proteins in the soluble fraction and pellet fraction were estimated separately by the Bradford method. Equal amounts (50 μg) of each sample were added with SDS polyacrylamide gel electrophoresis sample buffer and run in a 10% SDS–polyacrylamide gel. The sample was then analyzed by Western blotting and probed with the antibody against α -tubulin (1:1000 dilutions).

Assembly of Microtubules after Cold Treatment in TF Treated HeLa Cells. Assembly of the cold depolymerized microtubules of HeLa cells in the presence of TF (100, 150 $\mu\text{g}/\text{mL}$) was observed by immunofluorescence against α -tubulin using a Zeiss LSM 510 Meta confocal microscope. Cultured HeLa cells (1×10^5 cells/mL) were grown on glass coverslips for 24 h and then incubated at 4 $^{\circ}\text{C}$ for 6 h. After cold treatment, the cold medium was replaced with warm medium containing TF, and subsequently, the samples were incubated at 37 $^{\circ}\text{C}$ for 60 min. Cells were then fixed with 2% (v/v) paraformaldehyde at room temperature for 20 min. The fixed cells were then tagged with mouse monoclonal anti- α -tubulin antibody (1:200 dilutions) followed by anti-mouse rhodamine conjugated IgG antibody (1:150 dilutions) to visualize the reassembled microtubules and nucleus was stained with DAPI (1 $\mu\text{g}/\text{mL}$).

Purification of Tubulin from Goat Brain. Tubulin was isolated from goat brain by two cycles of temperature-dependent assembly and disassembly in PEM buffer (50 mM PIPES, 1 mM EGTA, and 0.5 mM MgCl_2 , pH 6.9) in the presence of 1 mM GTP, followed by two more cycles in 1 M glutamate buffer.²² Aliquots were flash-frozen in liquid nitrogen and stored at -70 $^{\circ}\text{C}$. The protein concentration was estimated by the method of Bradford²⁰ using bovine serum albumin as the standard.

Microtubule Polymerization. Tubulin (10 μM) was mixed with different concentrations of TF (10–100 $\mu\text{g}/\text{mL}$) in polymerization buffer (1 mM MgSO_4 , 1 mM EGTA, 1.0 M monosodium glutamate, pH 6.8) and polymerization reaction was initiated by adding 1 mM GTP in the reaction mixture at 37 $^{\circ}\text{C}$. The rate and extent of the polymerization reaction were monitored by light scattering at 350 nm using V-630 Jasco spectrophotometer connected to constant temperature water circulating bath.²³

Statistical Analysis. Data are presented as the mean of at least three independent experiments along with standard deviation (SD). Statistical analysis of data was done by Student's *t* test. Probability values (*p*) of <0.05 were considered to be statistically significant.

RESULTS

Theaflavins (TF) Inhibited Proliferation of HeLa Cells. To determine the effect of TF on the viability of HeLa cells, we performed MTT assay. HeLa cells were treated with varying concentrations of TF, i.e., 0, 25, 50, 100, 150, and 200 $\mu\text{g}/\text{mL}$ for 24 and 48 h. Treatment for 24 h did not change any significant amount in cell viability and about 80% cells were still viable at 200 $\mu\text{g}/\text{mL}$ dose of TF. But after 48 h of treatment a large amount of reduction in cell viability was observed (around 6.5–72%) in a dose dependent manner. The IC_{50} was found to be 110 ± 2.1 $\mu\text{g}/\text{mL}$ (*p* < 0.01) at 48 h (Figure 1).

TF Induced Cell Cycle Arrest in G_2/M Phase. To determine the possible antiproliferative mechanism of TF, we wanted to observe the cell cycle pattern of HeLa cells on TF treatment. Since treatment for 48 h caused cell death (as MTT assay shows), we did 24 h treatment with TF and cell cycle distribution pattern was analyzed by flow cytometer (Figure 2A). Treatment with 50 $\mu\text{g}/\text{mL}$ (below IC_{50} dose), 100 $\mu\text{g}/\text{mL}$ (near IC_{50} dose) and 150 $\mu\text{g}/\text{mL}$ (above IC_{50} dose) TF caused accumulation of 21.5%, 25.5%, and 29.7% cells, respectively, in G_2/M phase compared to 18.35% cells in the case of vehicle treated control. The average

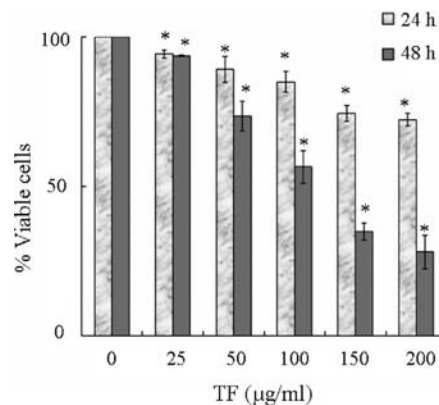


Figure 1. Effect of TF on the viability of HeLa cells (MTT assay). Cells were treated with TF (0–200 $\mu\text{g}/\text{mL}$) for 24 and 48 h. The data are shown as mean \pm SD (**p* < 0.05 compared to untreated control cells). The IC_{50} was calculated from three different experiments and found to be 110 ± 2.1 $\mu\text{g}/\text{mL}$ (*p* < 0.01) at 48 h.

histogram plot of cell cycle analysis (Figure 2B) indicates that the dose dependent increase in G_2/M phase population in presence of TF was mainly at the expense of G_0/G_1 population, compared to the control cells. A significant increase in S-phase population was also observed at 150 $\mu\text{g}/\text{mL}$ TF dose. Around 23.45% cells were accumulated in S-phase in the presence of 150 $\mu\text{g}/\text{mL}$ TF compared to 13.15% cells in control cells.

TF Increased Annexin V Positive Cell Population. To confirm apoptotic cell death induced by TF, annexin V-FITC and propidium iodide (PI) double staining for vehicle treated and TF treated HeLa cells was performed and analyzed by flow cytometry. Treatment with 50, 100, and 150 $\mu\text{g}/\text{mL}$ TF for 48 h increased the number of early apoptotic population (annexin V positive/PI negative) ranging from $6.4 \pm 1.7\%$ to $19.7 \pm 0.7\%$, over $2.2 \pm 0.9\%$ of the vehicle treated control (Figure 3A).

We have also observed increased fluorescence of annexin V-FITC positive apoptotic cells by confocal microscope with respect to nonapoptotic control cells (Figure 3B). This observation along with the increase in early apoptotic population could be explained by the fact that TF induced externalization of phosphatidylserine at early stage in apoptosis. These results clearly indicated that TF induced apoptosis in HeLa cells.

TF Induced Loss of Mitochondrial Membrane Potential ($\Delta\psi$) of HeLa Cells. Rhodamine 123 is a lipophilic cationic fluorescent dye, which is selectively taken up by mitochondria, and its uptake is directly proportional to the mitochondrial membrane potential ($\Delta\psi$) of cells,²⁴ making it an early marker of apoptosis. Treatment of HeLa cells with TF (50–150 $\mu\text{g}/\text{mL}$) for 48 h resulted in a dose-dependent loss of mitochondrial membrane potential (% MFI: 78.8%, 59.6% and 40.9%) in comparison to vehicle-treated cells (% MFI: 100%) (Figure 4A, 4B).

TF Altered the Expression of Proteins Involved in Apoptosis in HeLa Cells. Since TF caused cell death through apoptosis, we were interested to see the expression pattern of pro-apoptotic (p53, Bax and cleaved caspase-3) and antiapoptotic (Bcl-2) proteins after treatment of HeLa cells with TF (100 and 200 $\mu\text{g}/\text{mL}$) for 48 h (Figure 4C). Densitometry of immunoblot showed increased levels of p53, Bax and cleaved caspase-3 expression (up to 2.1-, 1.89-, and 2.8-fold, respectively) and decreased level of Bcl-2 expression (up to 0.19-fold) in TF treated cells compared to vehicle treated control HeLa cells. Here β -actin was used as the loading control.

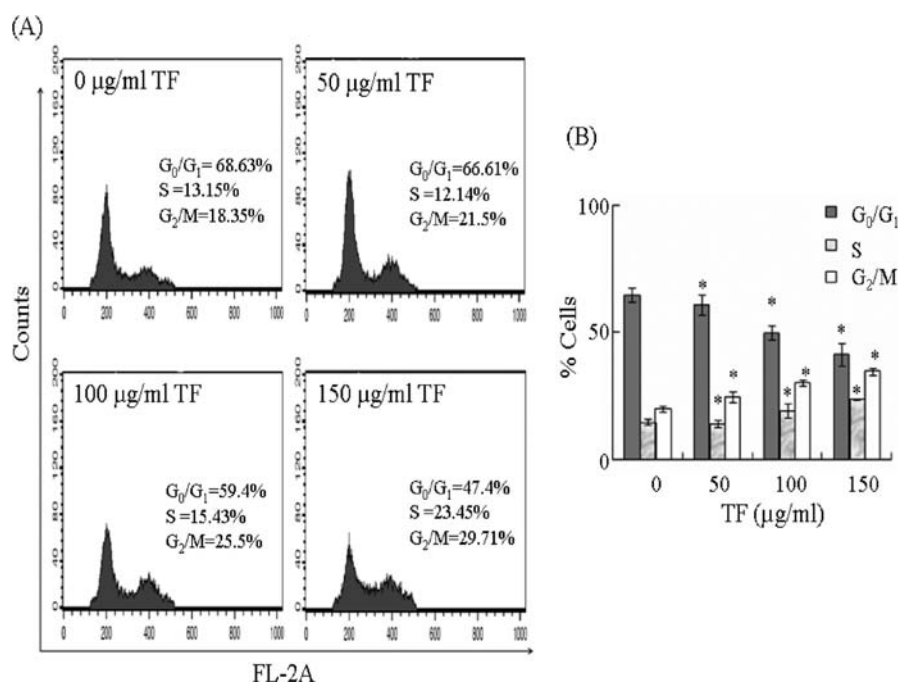


Figure 2. Analysis of cell cycle distribution of HeLa cells by flow cytometer. Cultured HeLa cells were treated with 0, 50, 100, and 150 µg/mL TF for 24 h. (A) Histogram analysis of one of the three experiments is shown. (B) Average distribution of cell cycle pattern was plotted which shows that the progress of cell cycle was arrested at G₂/M phase. The data represents three independent experiments and is shown as mean ± SD (* *p* < 0.05 compared to untreated control).

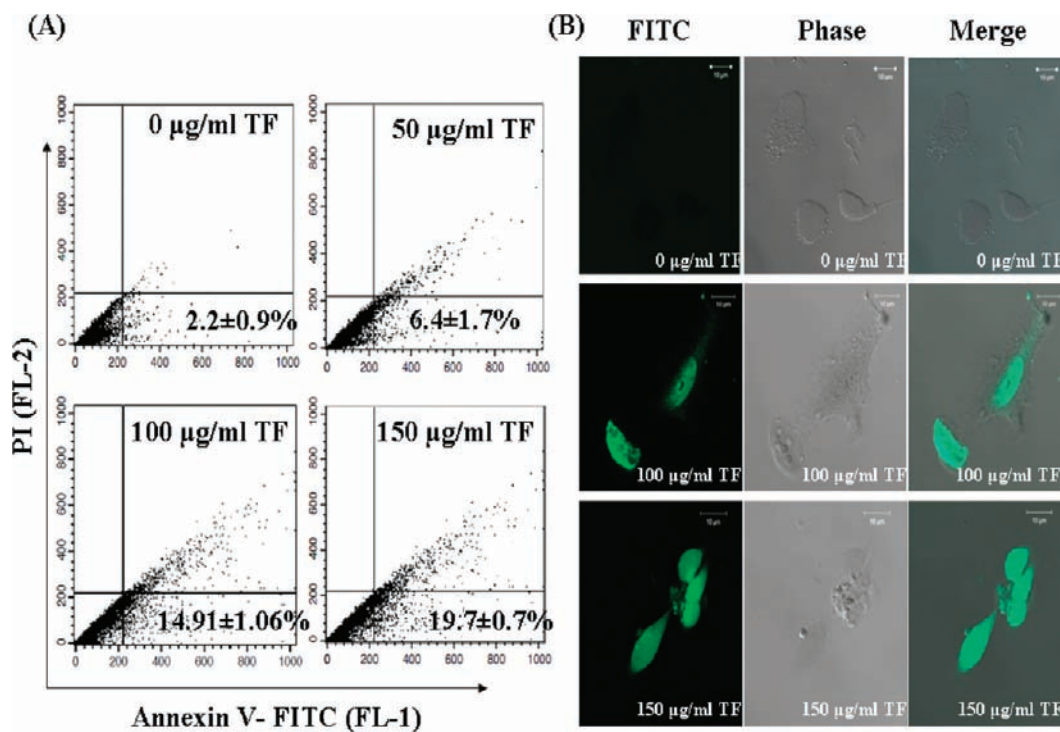


Figure 3. (A) Annexin V-FITC/PI assay for showing that TF induces apoptosis in HeLa cells. Untreated and TF treated (50, 100, and 150 µg/mL) cells were harvested after 48 h exposure and stained with annexin V-FITC and PI. The percentage of cells in the lower right quadrant is the measure of early apoptotic cells. The data represents three independent experiments with the mean ± SD (*n* = 3 culture plates). (B) Immunofluorescence study of annexin V-FITC positive apoptotic HeLa cells. Left panel shows the FITC fluorescence of untreated and TF treated cells, middle panel shows corresponding phase contrast images of the cells and the right panel shows the merged images. The doses of TF used are 0 µg/mL (upper row), 100 µg/mL (middle row) and 150 µg/mL (lower row). The experiments were performed thrice with similar results.

TF Altered Cellular Morphology of HeLa Cells. To see the effect of TF on cellular morphology, cultured HeLa cells were

treated with TF (50–150 µg/mL) for 24 h, and bright field images of control and TF treated cells were taken by Olympus

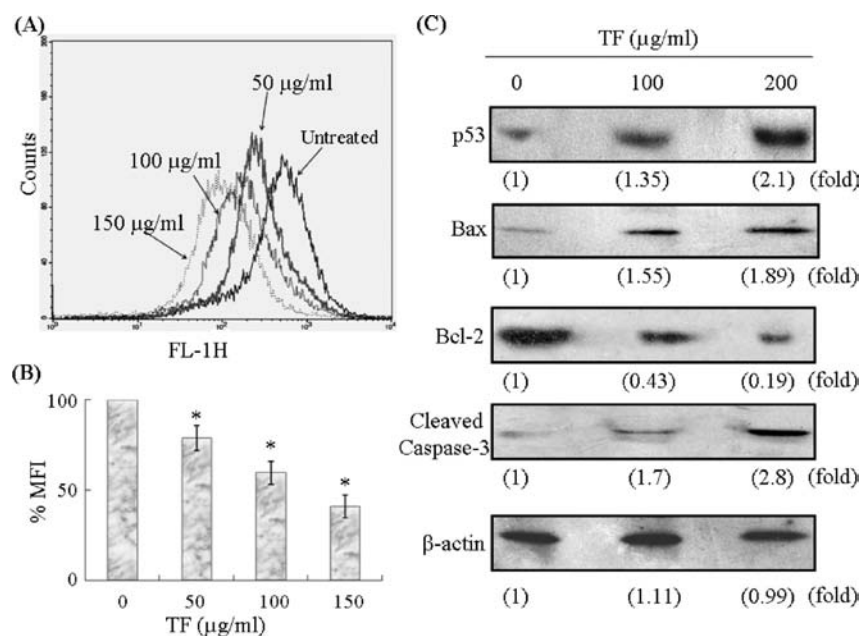


Figure 4. (A, B) Determination of mitochondrial membrane potential. Freshly isolated HeLa cells (1×10^6) treated with TF (50–150 µg/mL) for 48 h were stained with rhodamine 123 and incubated for 60 min, and its fluorescence was measured using a flow cytometer with an FL-1 filter. Results are expressed as a representative histogram (A) and a bar diagram of mean fluorescence intensity (MFI) (B) obtained from the histogram statistics (data represented as mean \pm SD, * $p < 0.05$ versus control). (C) Western blot analysis of p53, Bax, Bcl-2 and cleaved caspase-3 with densitometric analysis to show fold increased or decreased upon TF treatment. β -Actin was used as the loading control. The figures represent one of three independent experiments with similar results. Details of the experiment are given in the Materials and Methods.

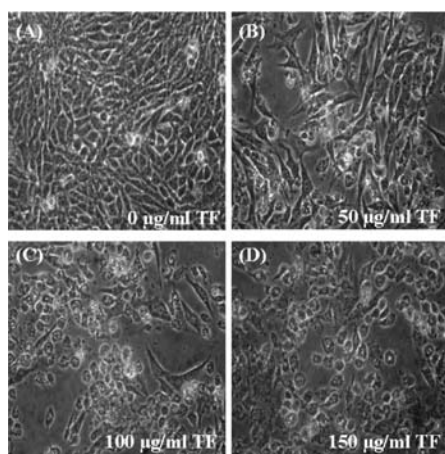


Figure 5. Alteration of morphology of HeLa Cells by TF. Bright field images of untreated and TF treated HeLa cells were taken by Olympus inverted microscope model CKX41. A, B, C and D represent HeLa cells treated with 0, 50, 100, and 150 µg/mL TF, respectively.

inverted microscope model CKX41. Figure 5A shows the morphology of vehicle treated control cells. Cell morphology was changed at 50 µg/mL TF (Figure 5B), and the cells became smaller in size and more round-shaped in presence of 100 µg/mL (Figure 5C) and 150 µg/mL TF (Figure 5D). Since cellular microtubule network maintains cell cytoskeleton, alteration in cell morphology might be due to disruption of this microtubule network.

TF Disrupted Microtubule Network in HeLa Cells. Since TF induced cell cycle arrest in G_2/M phase and also effectively altered the cellular morphology of HeLa cells, we were interested to know whether TF altered the microtubule network inside the cells. This was examined by confocal microscopy (Figure 6).

Control HeLa cells (Figure 6A) showed typical interphase microtubule organization. However, 50 µg/mL TF (Figure 6B) caused significant change of microtubule structure with reduced microtubule at periphery. Higher doses of TF (100 and 150 µg/mL) drastically disrupted the central microtubule network (Figure 6C,D). These results indicated that TF might have depolymerized cellular microtubule.

TF Reduced the Polymerized Microtubule Mass in HeLa Cells. To quantify the effect of TF on microtubule mass in HeLa cells, Western blot analysis was performed for the soluble tubulin and the assembled tubulin of TF treated HeLa cells. Treatment of cells with 100 and 150 µg/mL TF for 24 h increased the level of soluble tubulin and decreased the level of polymeric tubulin (Figure 6E, lanes 2, 3) compared to that in vehicle treated control cells (Figure 6E, lane 1), while the total amount of tubulin remains unchanged. These results showed a pattern similar to that of colchicine, a microtubule-depolymerizing agent (positive control, Figure 6E, lane 4). This result clearly indicated that TF depolymerized cellular microtubule in HeLa cells.

TF Suppressed the Reassembly of Cold-Depolymerized Microtubules in HeLa Cells. To know whether TF affected the cellular microtubule formation, we examined the reassembly pattern of depolymerized microtubule in the presence and absence of TF. Cellular microtubules were depolymerized by incubating HeLa cells at 4 °C for 3 h (until the morphology of the cells appeared round). Subsequently, the reassembly kinetics of microtubules in those cells was monitored by incubating the cells with fresh warm media containing different concentrations of TF at 37 °C (Figure 7). Cells before cold treatment showed normal interphase microtubule structure (Figure 7A), and after incubation in the cold for 3 h, cells became contracted with depolymerized microtubule structure (Figure 7B). In the absence of TF, cold-depolymerized interphase microtubules reassembled to

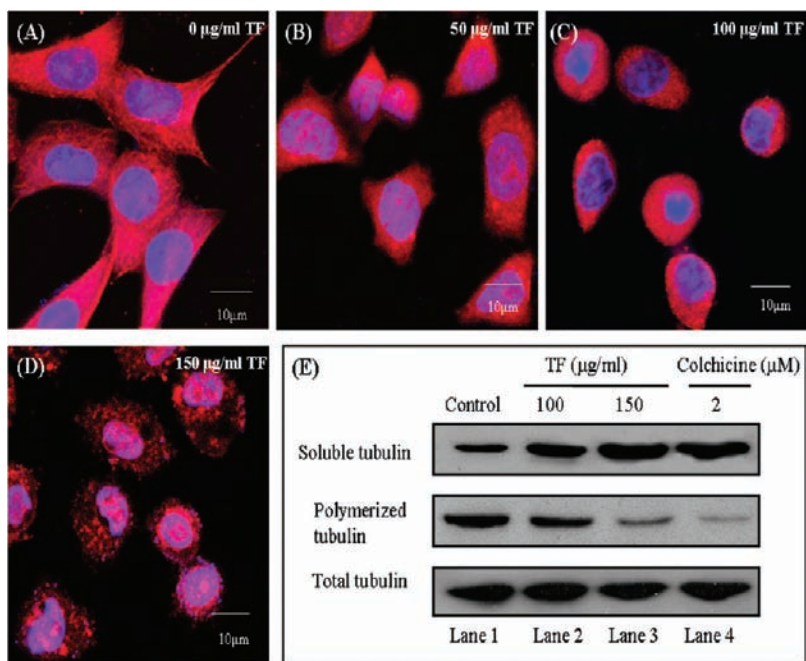


Figure 6. Immunofluorescence study of disruption of interphase microtubules of HeLa cells treated with TF. A, B, C and D are HeLa cells treated with 0, 50, 100, and 150 $\mu\text{g/ml}$ TF, respectively, for 24 h. Microtubules were tagged with rhodamine (red), and nucleus was stained with DAPI (blue). Images were taken under confocal microscope. Experiments were repeated thrice with similar results. (E) Effect of TF on tubulin polymerization in HeLa cells. HeLa cells were treated with 0, 100, and 150 $\mu\text{g/ml}$ TF for 24 h. Following cell lysis, the polymerized and soluble form of tubulin was separated by centrifugation. Western blot analysis was conducted using an antibody against α -tubulin.

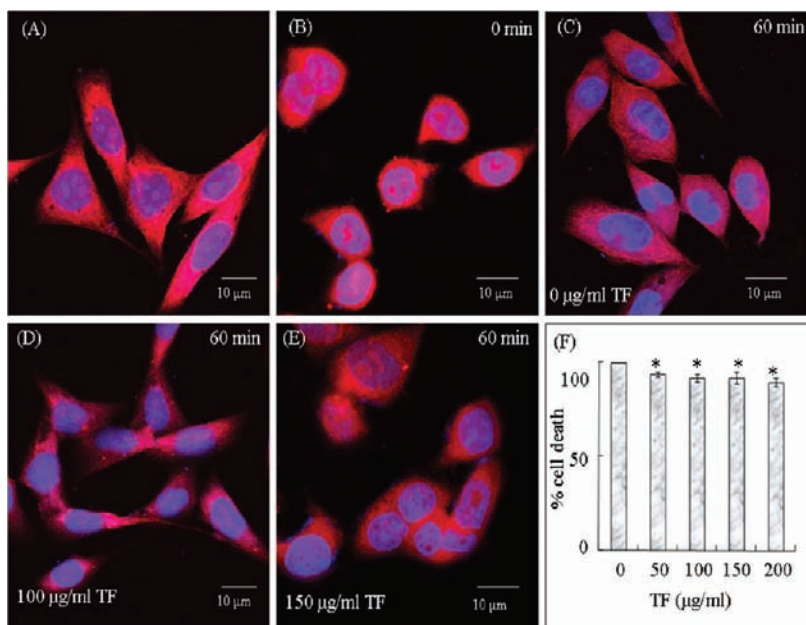


Figure 7. Immunofluorescence study of reassembly pattern of cold depolymerized interphase microtubule after replacement with warm media and incubation. A and B represent HeLa cells before cold treatment and HeLa cells immediate after cold treatment, respectively. (C–E) The reassembly pattern of interphase microtubules of untreated (C), 100 $\mu\text{g/ml}$ (D) and 200 $\mu\text{g/ml}$ (E) TF treated HeLa cells after incubation for 60 min with warm media. Microtubules were tagged with rhodamine (red), and nucleus was stained with DAPI (blue). (F) MTT assay performed with cold treated HeLa cells in presence of 0, 50, 100, 150, and 200 $\mu\text{g/ml}$ TF after an incubation period of 60 min. Result shows only about 10% cells are dead even after treatment with 200 $\mu\text{g/ml}$ TF. Experiments were repeated thrice with similar results and expressed as mean \pm SD (* $p < 0.05$).

form normal microtubule network within 60 min of incubation at 37 $^{\circ}\text{C}$ with fresh media (Figure 7C). In the presence of 100 $\mu\text{g/ml}$ TF, the reassembly of interphase microtubule was just started after 60 min of incubation (Figure 7D). However, in the

presence of 150 $\mu\text{g/ml}$ TF, microtubules failed to reassemble after 60 min of incubation at 37 $^{\circ}\text{C}$ (Figure 7E). To know whether treatment with TF after 3 h of cold shock had any drastic effect on cell viability, we performed MTT assay. HeLa cells were incubated at

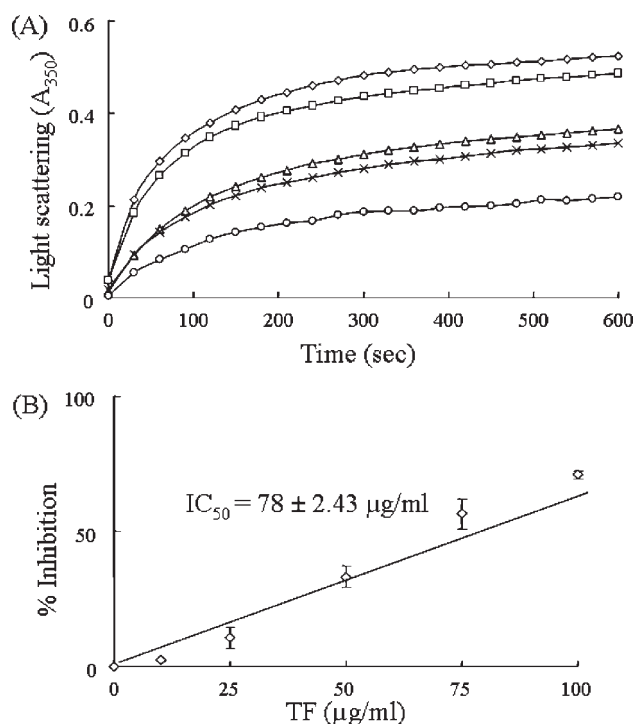


Figure 8. Inhibition of tubulin assembly by TF *in vitro*. (A) One of the three individual experiments showing the effect of TF on microtubule polymerization kinetics, assessed by monitoring the increase in light scattering at 350 nm. Different TF concentrations are as follows: control (\diamond), 25 $\mu\text{g/mL}$ (\square), 50 $\mu\text{g/mL}$ (\triangle), 75 $\mu\text{g/mL}$ (\times) and 100 $\mu\text{g/mL}$ (\circ). (B) Percent of inhibition of polymerization with respect to the increase in concentration of TF with calculated IC_{50} value.

4 $^{\circ}\text{C}$ for 3 h, then the cold media was replaced with fresh warm media and treatment was given with TF (0–200 $\mu\text{g/mL}$) for 1 h at 37 $^{\circ}\text{C}$. The result (Figure 7F) showed that only around 10% cells were dead even at 200 $\mu\text{g/mL}$ dose of TF. This data demonstrated that treatment of the cold treated HeLa cells with TF for 1 h did not alter significant cell viability but effectively prevented the polymerization on tubulin into microtubule.

TF Inhibited Tubulin Polymerization, *in Vitro*. The effect of TF on tubulin polymerization, *in vitro*, was examined using purified tubulin by light scattering assay. Purified tubulin (10 μM) was polymerized in the absence or presence of different concentrations of TF (10–100 $\mu\text{g/mL}$), and the results of such experiments are shown in Figure 8. TF inhibited the rate and the extent of tubulin polymerization in a concentration dependent manner (Figure 8A). The IC_{50} value (50% inhibition of microtubule polymerization) was calculated from a plot of percent of inhibition against doses of TF in MS Excel taking the control (polymerization in absence of TF) as zero percent. The IC_{50} occurred at TF concentration (IC_{50}) of $78 \pm 2.43 \mu\text{g/mL}$ ($P < 0.01$) (Figure 8B).

DISCUSSION

The tubulin—microtubule system is one of the most successful targets for cancer chemotherapy, and it has been used for screening and development of potential anticancer drugs.^{25,26} Here we demonstrated the antiproliferative activity of theaflavins (TF) through G_2/M arrest and apoptosis in relation to depolymerization of microtubule in cervical carcinoma HeLa cells. The cellular results were then validated by *in vitro* experiments, where we found that TF inhibited tubulin polymerization.

We tested the antiproliferative activity of TF by MTT assay and found that TF inhibited the growth of HeLa cells effectively in 48 h with IC_{50} occurring $110 \pm 2.1 \mu\text{g/mL}$ (Figure 1), which was in agreement with previous studies demonstrating a wide range of growth inhibitory effect of TF on various cancer cell lines.^{27,28} On the basis of this finding, we decided to find out the mechanism of cell death caused by TF treatment. We performed cell cycle analysis and found that TF caused G_2/M arrest of HeLa cell cycle. Previous studies reported that TF induced apoptosis in various human cancer cells.^{1,2,4} Since there was no report on the effect of TF on HeLa cells, we investigated whether TF caused apoptosis in HeLa cells. In our study, we observed that TF increased apoptotic population in HeLa cells within 48 h in a dose dependent manner (Figure 3), suggesting that viability inhibition of HeLa cells might be due to both cell cycle arrest and induction of apoptosis. To confirm TF-induced apoptosis in HeLa cells we observed the expression pattern of antiapoptotic and proapoptotic proteins of Bcl-2 family. We found upregulation of proapoptotic protein Bax and downregulation of antiapoptotic protein Bcl-2 (Figure 4C), suggesting that the increased ratio of Bax:Bcl-2 might induce apoptosis.²⁹ Activation of Bax leads to its translocation into mitochondria and increases the permeability of mitochondrial membrane. This causes loss of mitochondrial membrane potential, which in turn releases cytochrome *c* into the cytosol. Released cytochrome *c* can activate caspase-9, and activated caspase-9, in turn, cleaves and activates executioner caspase-3.^{30,31} In our study, a gradual loss of mitochondrial membrane potential (MMP) was observed in HeLa cells after 48 h of treatment with TF (Figure 4A,B). This loss of MMP was also accompanied by activation of cleaved caspase-3 as measured by Western blot analysis (Figure 4C). We also observed the upregulation of proapoptotic protein p53 in TF treated HeLa cells.

Next, our intention was to find out a cellular target of TF in HeLa cells. Since TF arrested cell cycle in G_2/M phase and many microtubule targeted anticancer compounds induce G_2/M arrest,^{15–17} we became interested to investigate the interaction of TF with cellular microtubules of HeLa cells and also with purified tubulin in cell free system. We observed that treatment with TF resulted in cellular morphology change (Figure 5) with disruption of microtubule structure within 24 h, even at a lower dose of TF (50 $\mu\text{g/mL}$) (Figure 6). The fibrous structure of vehicle treated control HeLa cells was found to be depolymerized within 24 h of treatment with 50, 100, and 150 $\mu\text{g/mL}$ TF, whereas with these doses no significant cell death was observed within that time period. Moreover, although 50 $\mu\text{g/mL}$ dose of TF caused no significant cell death after 24 h, that dose was sufficient to initiate microtubule disruption within that time period. We also found that 24 h of treatment with TF increased the soluble tubulin fraction and decreased the polymerized microtubule fraction in HeLa cells whereas the total tubulin content was same (Figure 6E). This data strongly supports that TF depolymerizes cellular microtubule inside HeLa cells much before the onset of apoptosis. Since tubulin is an important cytoskeletal protein participating in various cellular processes and disruption of the cellular microtubule network leads to apoptosis,^{32,33} it can be concluded from our data that disruption of microtubule network might be one of the causes of TF-induced apoptosis in HeLa cells. The upregulation pattern of proapoptotic protein p53 in TF treated HeLa cells was very significant because similar trends were reported when cultured mammalian cells were treated with microtubule targeted

drugs.^{34,35} Disruption of microtubule structure by TF led us to investigate the effect of TF on the temperature dependent reassembly of tubulin into microtubule in HeLa cells. We showed that incubation of cells for 1 h with TF near IC₅₀ doses (100 and 150 µg/mL) prevented reassembly of cold depolymerized microtubule, whereas the treatment did not affect the cell viability significantly (Figure 7). This data again demonstrated that disruption of microtubule structure might be due to depolymerization of cellular microtubule. So, to test this we observed the polymerization of purified tubulin, *in vitro*, in the presence of TF and we found that glutamate induced tubulin polymerization into microtubule was inhibited by TF in a concentration dependent manner (Figure 8).

Briefly, we can conclude that disruption of microtubule network by depolymerization of microtubule mass in HeLa cells by TF can cause cell cycle arrest at G₂/M phase and activate mitochondrial pathway of apoptosis by changing the Bax/Bcl-2 ratio and activation of p53. Our finding shows cellular cytoskeleton protein tubulin as one of the novel targets of TF, and that may cause cell cycle arrest and apoptosis in HeLa cells. Theaflavins could be used in combination with other microtubule targeted drugs for treatment of cancer, and it also might be used as a lead compound for development of potential antimicrotubule agent for cancer therapy.

AUTHOR INFORMATION

Corresponding Author

*Department of Biotechnology and Dr. B. C. Guha Centre for Genetic Engineering and Biotechnology, University of Calcutta, 35 Ballygunge Circular Road, Kolkata-700 019, WB, India. Tel: 91-33-2461-5445. Fax: 91-33-2461-4849. E-mail: gcbcg@caluniv.ac.in.

Funding Sources

The work was supported by grants from BRNS/DAE, Govt. of India (No. 2006/37/21/BRNS), DST, Govt. of India (No. SR/SO/BB-14/2008), and DBT, Govt. of India (No. BT/PR12889/AGR/36/624/2009), to G.C. Confocal microscope and FACS facilities are developed by the grant from National Common Minimum Program, Govt. of India. S.C. is supported by a fellowship from UPE, University Grant Commission, and A.D. is supported by a fellowship from Calcutta University.

ABBREVIATIONS USED

TF, theaflavins; DAPI, 4',6-diamidino-2-phenylindole; FITC, fluorescein isothiocyanate; PI, propidium iodide; PBS, phosphate buffered saline; ELISA, enzyme-linked immunosorbent assay.

REFERENCES

- (1) Yang, G. Y.; Liu, Z.; Seril, D. N.; Liao, J.; Ding, W.; Kim, S.; Bondoc, F.; Yang, C. S. Black tea constituents, theaflavins, inhibit 4-(methylnitrosoamino)-1-(3-pyridyl)-1-butanone (NNK)-induced lung tumorigenesis in A/J mice. *Carcinogenesis* **1997**, *18*, 2361–2365.
- (2) Weisburger, J. H.; Rivenson, A.; Reinhardt, J.; Aliaga, C.; Braley, J.; Pittman, B.; Zang, E. Effect of black tea on azoxymethane induced colon cancer. *Carcinogenesis* **1998**, *19*, 229–232.
- (3) Goldbohm, R. A.; Hertog, M. G. L.; Brants, H. A. M.; van Poppel, G.; van den Brandt, P. A. Consumption of black tea and cancer risk: a prospective cohort study. *J. Natl. Cancer Inst.* **1996**, *88*, 93–100.
- (4) Katiyar, S. K.; Mukhtar, H. Tea in chemoprevention of cancer: epidemiologic and experimental studies (review). *Int. J. Oncol.* **1996**, *8*, 221–238.

- (5) Lu, Y. P.; Lou, R.; Xie, J. G.; Yen, P.; Huang, M. T.; Conney, A. H. Inhibitory effects of black tea on the growth of established skin tumor size, apoptosis, mitosis and bromodeoxyuridine incorporation into DNA. *Carcinogenesis* **1997**, *18*, 2163–2169.

- (6) Yang, G. Y.; Liao, Z.; Li, C.; Chung, Z.; Yurkow, E. J.; Ho, C. T.; Yang, C. S. Effect of black and green tea polyphenols on c-jun phosphorylation and H₂O₂ production in transformed and non-transformed human bronchial cell lines: possible mechanism of cell growth inhibition and apoptosis induction. *Carcinogenesis* **2000**, *21*, 2035–2039.

- (7) Halder, B.; Bhattacharya, U.; Mukhopadhyay, S.; Giri, A. K. Molecular mechanism of black tea polyphenols induced apoptosis in human skin cancer cells: involvement of Bax translocation and mitochondria mediated death cascade. *Carcinogenesis* **2008**, *29*, 129–138.

- (8) Jia, X. D.; Han, C.; Chen, J. S. Tea pigments induce cell-cycle arrest and apoptosis in HepG2 cells. *World J. Gastroenterol.* **2004**, *11*, 5273–5276.

- (9) Prasad, S.; Kaur, J.; Roy, P.; Kalra, N.; Shukla, Y. Theaflavins induce G₂/M arrest by modulating expression of p21^{waf1/cip1}, cdc25C and cyclin B in human prostate carcinoma PC-3 cells. *Life Sci.* **2007**, *81*, 1323–1331.

- (10) McIntosh, J. R.; Grishchuk, E.; West, R. R. Chromosome–microtubule interactions during mitosis. *Annu. Rev. Cell. Dev. Biol.* **2002**, *18*, 193–219.

- (11) Gunderson, G. G.; Cook, T. A. Microtubules and signal transduction. *Curr. Opin. Cell. Biol.* **1999**, *11*, 81–94.

- (12) Wilson, L.; Panda, D.; Jordan, M. A. Modulation of microtubule dynamics by drugs: a paradigm for the actions of cellular regulators. *Cell. Struct. Funct.* **1999**, *24*, 329–335.

- (13) Panda, D.; Jordan, M. A.; Chu, K. C.; Wilson, L. Differential effects of vinblastine on polymerization and dynamics at opposite microtubule ends. *J. Biol. Chem.* **1996**, *271*, 29807–29812.

- (14) Jordan, M. A.; Wilson, L. Microtubules as a target for anticancer drugs. *Nat. Rev. Cancer* **2004**, *4*, 253–265.

- (15) Jordan, M. A. Mechanism of action of antitumor drugs that interacts with microtubules and tubulin. *Curr. Med. Chem.: Anti-Cancer Agents* **2002**, *2*, 1–17.

- (16) Jordan, M. A.; Thrower, D.; Wilson, L. Mechanism of inhibition of cell proliferation by Vinca alkaloids. *Cancer Res.* **1991**, *51*, 2212–2222.

- (17) Acharya, B. R.; Choudhury, D.; Das, A.; Chakrabarti, G. Vitamin K3 disrupts the microtubule networks by tubulin binding: A novel mechanism of its anti-proliferative activity. *Biochemistry* **2009**, *48*, 6963–6974.

- (18) Mosmann, T. Rapid colorimetric assay for cellular growth and survival: application to proliferation and cytotoxic assays. *J. Immunol. Methods* **1983**, *65*, 55–63.

- (19) Events, A. M.; Prachand, S.; Shi, B. Imexon-induced apoptosis in multiple myeloma tumor cells is caspase-8 dependent. *Clin. Cancer Res.* **2004**, *10*, 1481–1491.

- (20) Bradford, M. M. A rapid and sensitive method for the quantitation of microgram quantities of protein utilizing the principle of protein-dye binding. *Anal. Biochem.* **1976**, *72*, 248–254.

- (21) Minnoti, A. M.; Barlow, S. B.; Cabral, F. Resistance to anti-mitotic drugs in chinese hamster ovary cells correlates with changes in the level of polymerized tubulin. *J. Cell Biochem.* **1991**, *266*, 3987–3994.

- (22) Hamel, E.; Lin, C. M. Glutamate-induced polymerization of tubulin: characteristics of the reaction and application to the large-scale purification of tubulin. *Arch. Biochem. Biophys.* **1981**, *209*, 29–40.

- (23) Gaskin, F.; Cantor, C. R.; Shelanski, M. L. Turbidimetric studies of the *in vitro* assembly and disassembly of porcine neurotubules. *J. Mol. Biol.* **1974**, *89*, 737–755.

- (24) Scaduto, R. C., Jr.; Grotyohann, L. W. Measurement of mitochondrial membrane potential using fluorescent rhodamine derivatives. *Biophys. J.* **1999**, *76*, 469–477.

- (25) Chakrabarti, G.; Sengupta, S.; Bhattacharyya, B. Thermodynamics of Colchicinoid-Tubulin Interactions role of B ring and C7 substituent. *J. Biol. Chem.* **1996**, *271*, 2897–2901.

(26) Pyles, A. E.; Bane, S. H. Effect of the B ring and the C-7 substituent on the kinetics of colchicinoid-tubulin associations. *Biochemistry* **1993**, *32*, 2329–2336.

(27) Friedman, M.; Mackey, B. E.; Kim, H. J.; et al. Structure–activity relationships of tea compounds against human cancer cells. *J. Agric. Food Chem.* **2007**, *55*, 243–253.

(28) Babich, H.; Pinsky, S. M.; Muskin, E. T.; Zuckerbraun, H. L. In vitro cytotoxicity of a theaflavin mixture from black tea to malignant, immortalized and normal cells from the human oral cavity. *Toxicol. In Vitro* **2006**, *20*, 677–688.

(29) Shroff, E. H.; Snyder, C.; Chandel, N. S. Role of bcl-2 family members in anoxia induced cell death. *Cell Cycle* **2007**, *6*, 807–809.

(30) Li, P.; Nijhawan, D.; Budihardjo, I.; Srinivasula, S. M.; Ahmad, M.; Alnemri, E. S.; Wang, X. Cytochrome c and dATP dependent formation of Apaf-1/caspase-9 complex initiates an apoptotic protease cascade. *Cell* **1997**, *91*, 479–489.

(31) Pan, G., Humke, E. W., Dixit, V. M. (1998) Activation of caspases triggered by cytochrome c in vitro. *FEBS Lett.* **1998**, *426*, 151–154.

(32) Mi, L.; Xiao, Z.; Hood, B. L.; Dakshanamurthy, S.; Wang, X.; Govind, S.; Conrads, T. P.; Veenstra, T. D.; Chung, F. L. Covalent binding to tubulin by isothiocyanates. A mechanism of cell growth arrest and apoptosis. *J. Biol. Chem.* **2008**, *283*, 22136–22146.

(33) Jordan, M. A.; Wilson, L. Microtubules and actin filaments: dynamic targets for cancer chemotherapy. *Curr. Opin. Cell Biol.* **1998**, *10*, 123–130.

(34) Sablina, A. A.; Chumakov, P. M.; Levine, A. J.; Kopnin, B. P. p53 activation in response to microtubule disruption is mediated by integrin-Erk signaling. *Oncogene* **2001**, *22*, 899–909.

(35) Stewart, Z. A.; Tang, L. J.; Pietenpol, J. A. Increased p53 phosphorylation after microtubule disruption is mediated in a microtubule inhibitor and cell specific manner. *Oncogene* **2001**, *20*, 113–124.